

Article

Thermal, Photometric and Radiometric Properties of Multi-Color LEDs Situated on the Common PCB [†]

Krzysztof Górecki *  and Przemysław Ptak 

Department of Marine Electronics, Gdynia Maritime University, Morska 81-87, 81-225 Gdynia, Poland;
p.ptak@we.umg.edu.pl

* Correspondence: k.gorecki@we.umg.edu.pl; Tel.: +48-58-5586448

[†] This paper is an extended version of our paper published in Proceedings of the 25th International Workshop on Thermal Investigations of ICs and Systems Thermic 2019, Lecco, Italy, 27–29 September 2019, doi:10.1109/THERMINIC.2019.8923416.

Received: 16 September 2020; Accepted: 10 October 2020; Published: 13 October 2020



Abstract: This paper presents the results of experimental investigations illustrating the influence of the spectra of the light emitted by power LEDs on their thermal, photometric and radiometric parameters. The investigations were performed for six diodes emitting white or monochromatic light of different spectra. Each of these diodes was produced by the same manufacturer, mounted in the same package and the tested devices were soldered to the common PCB. In the paper, the manner and set-ups making possible measurements of self and transfer transient thermal impedances, illuminance and the surface power density of the light emitted by the tested devices are described. Selected results of measurements are shown and discussed. These results prove that the spectra of the emitted light influence self-transient thermal impedances of the considered devices and transfer transient thermal impedances between some pairs of these devices. Additionally, it is proved that thermal couplings between the tested diodes strongly influence their junction temperature and the surface power density of the emitted radiation.

Keywords: color and white power LEDs; thermal parameters; radiometric parameters; self-heating; mutual thermal couplings

1. Introduction

Currently, power LEDs emitting light of different colors are easily accessible. The light emitted by these devices is characterized by different spectra and each color is connected with the definite wavelength of the emitted light [1–3]. In the literature, one can find a lot of information on investigations concerning the considered class of diodes emitting white light used in the lighting technique [4–6]. Additionally, some papers refer to diodes emitting monochromatic light [7–9].

In the paper [10], RGB LEDs with monolithically integrated photodetectors are proposed. Such structures are used to control the color coordinates of RGB LEDs. The paper [11] proposes precise dimming and color control of an LED system. This system uses a bicolor adjustable LED lamp and makes it possible to precisely control CCT (correlated color temperature) and radiance. In the paper [12], the method of controlling the luminous intensity and CCT of a lighting system including white power LEDs is proposed. Analytical dependences describing the mentioned parameters of such a system are formulated and discussed.

The paper [13] presents equations describing the influence of the diode internal temperature and electrical power dissipated in the diode on luminous efficiency and luminous flux. The mentioned dependences have the form of a polynomial of the second or third order. Additionally, a manner of determining the value of the heating power is proposed in the cited paper. Using the proposed

dependences, it was shown how to estimate the value of the diode forward current, at which the emitted luminous flux has the maximum value. In the paper [14], a dynamic version of the description of power LED properties given in the paper [13] is proposed. The proposed equations make it possible to calculate waveforms of luminous efficiency and the internal temperature of power LEDs operating continuously in typical lighting systems or operating in the switched mode, for example, in traffic lights.

In the paper [15], a method of measuring the internal temperature of power LEDs is proposed. This method is based on the general photo-electro-thermal theory for LED systems and the coefficient characterizing the reduction of luminous efficiency with junction temperature. Good agreement between the results of the measurements obtained with the proposed method and the data given by the producers of different types of LEDs is achieved.

The papers [16,17] present the theory and photo-electro-thermal model of phosphor-coated LEDs. Apart from the properties of the LED structure, the dynamic properties of phosphor coating used in power LEDs to obtain white light are also taken into account. The results illustrating the correctness of the proposed model are shown and commented upon. In the paper [18], some results of analyses performed with the use of such a model are compared with the results of dynamic measurements.

As it is commonly known, junction temperature strongly influences the properties of semiconductor devices, for example, power LEDs [3,4,6,19–24] and electronic networks [25,26]. The value of this temperature is higher than the ambient temperature due to self-heating phenomena and mutual thermal couplings between devices situated on the common PCB or a heat-sink. The value of junction temperature increases with an increase in thermal power dissipated in the considered device and it depends also on the efficiency of removal of the heat generated in this device to the surroundings [4,6,27]. This efficiency could be characterized, for example, by thermal resistance or transient thermal impedance.

The influence of the device internal temperature on the electrical and optical properties of the considered devices is very important [6,27–30]; also an increase in the device internal temperature considerably shortens the lifetime of these devices [5,31–33]. Another important problem is the thermal management of power LEDs. As it is shown in the paper [5], an increase in the diode temperature equal to 20 °C can cause even a six-time decrease of its lifetime.

To characterize the thermal properties of semiconductor devices situated on the common PCB, transfer transient thermal impedances are additionally used [6,34–36]. While measuring these parameters, the efficiency of the conversion of electrical energy into light is of essential significance, and it depends on the colors of the emitted light [3,37].

On the other hand, optical properties of power LEDs are characterized by, for example, illuminance and the surface power density on the surface illuminated by these devices [3,38]. In our previous papers [26,36,37], the method of measuring thermal and optical parameters of power LEDs is described, but its usefulness was verified only for LEDs emitting white light.

LEDs emitting light of different colors are made of various semiconductor materials [3]. Each such material is characterized by specific values of material parameters, for example, band-gap voltage. They are also characterized by a narrower spectrum characteristic of the emitted light than power LEDs emitting white light [3,21]. Generally, photometric parameters characterize properties of the observed light taking into account the properties of the human eye. Due to differences between the spectrum characteristics of the considered color power LEDs with the same value of surface power density as the emitted lighting, different values of illuminance measured in the same distance from the tested diode can be observed [3].

The manufacturer of the considered class of semiconductor devices typically gives information about the properties of these devices obtained at quasi-ideal operating conditions. In the characteristics of power LEDs presented in the catalog data, the influence of such phenomena as self-heating or mutual thermal couplings with other devices on the properties of these power LEDs is usually omitted. In order to characterize the properties of the considered devices operating in real conditions, some measurements should be performed. On the other hand, the authors could not find in the

literature any systematic study describing the influence of self-heating and mutual thermal couplings on thermal and optical properties of power LEDs situated in the same packages and soldered to the common PCB.

The aim of this paper, which is an extended version of the paper [39], is to investigate the influence of the spectra of the emitted light on the electrical, thermal, photometric and radiometric parameters of white and color power LEDs situated on the common PCB. Set-ups indispensable to measuring the mentioned parameters were designed and constructed. Measurements were performed for power LEDs situated in identical cases and emitting light of selected colors or white light of different CCT. The results of measurements obtained for the tested devices at different operating conditions are compared and discussed. In comparison with the paper [39], we extended the description of the investigated diodes, the used measurement set-ups and the measurement methods. This paper contains new results of investigations that were performed for a bigger number of tested devices than in the paper [39]. The new results of measurements illustrate the influence of self-heating phenomena and mutual thermal couplings between the tested devices on their optical and thermal properties.

In Section 2, the tested devices are described. Section 3 presents the used measurement set-ups. The results of the measurements are shown and discussed in Section 4.

2. Tested Devices

We performed measurements for four colored and two white power LEDs by OSRAM Semiconductor [37]. Each of these diodes emits light of different colors: LW (White), LCW (Warm White), LB (Blue), LT (Green), LY (Yellow) and LR (Red). We selected such diodes taking into account the following reasons:

- (a) they are manufactured by a famous company,
- (b) all the diodes are mounted in cases of the same type,
- (c) they emit light typically used in such popular applications as hospitality, mood lighting, stage lighting, table lamp, signaling in cars and planes (for white, yellow and red LEDs), transportation, planes and ships (for green and blue LEDs).

According to the data given by the producer [40], the maximum allowable forward current of these diodes amounts to 1 A, whereas the viewing angle is equal to 120°. The maximum admissible junction temperature of these diodes is 135 °C. Table 1 contains values of the total luminous flux Φ_V , thermal resistance R_{thj-s} between the junction and the soldering point and dominant wavelength λ_{max} for all the tested LEDs.

Table 1. Values of selected exploitation parameters of the tested LEDs.

Diode	LR	LY	LT	LB	LW	LCW
R_{thj-s} (K/W)	6.5	6.5	6.5	5	5	5
Φ_V (lm)	39–71	39–82	52–97	15–33	71–130	45–97
	@ 400 mA	@ 400 mA	@ 350 mA	@ 350 mA	@ 350 mA	@ 350 mA
λ_{max} (nm)	628	590	528	467	536	610

The total luminous flux changes from 15 lm for a blue diode to 130 lm for a white diode at forward current equal to 0.35 or 0.4 A. The different values of forward current, at which the value of the luminous flux is measured, are given by the manufacturer. It is also worth noticing that for two diodes of the same type one can obtain values of Φ_V which differ even twice as much. The producer gives in the catalog data the information on the minimum and maximum value of the emitted luminous flux of the considered types of power LEDs and additionally defines four models of each type of the investigated diodes. Each of these models is characterized by the value of the emitted luminous flux from a range four times narrower than the range given in Table 1. The thermal resistance of these diodes between the junction and the soldering point falls in a range from 5 to 6.5 K/W [40]. Different values of

R_{thj-s} prove that the properties of the semiconductor material used to produce the considered diodes can cause a change in the value of the considered parameter even by 30%. Additionally, it is apparent that the phosphor coating used in LEDs emitting white light practically does not influence the value of R_{thj-s} . Values of the dominant wavelength λ_{max} fall in a range from 467 nm to 628 nm. According to the information given by the producer diodes, LCW, LB, LT and LW are made of GaN, whereas the diodes LY and LR are made of InGaAlP [40].

The view of the case of the considered power LEDs is shown in Figure 1 [41]. This case has the dimensions, $7.2 \times 6.2 \times 1.9$ mm. It is visible that this case contains a thermal pad, which makes it possible to reduce the thermal resistance of the tested diodes [42].

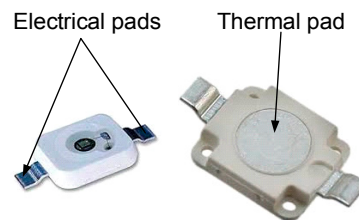


Figure 1. View of the top and bottom sides of the case of the tested LEDs.

Relative emission spectra of the considered power LEDs are shown in Figure 2.

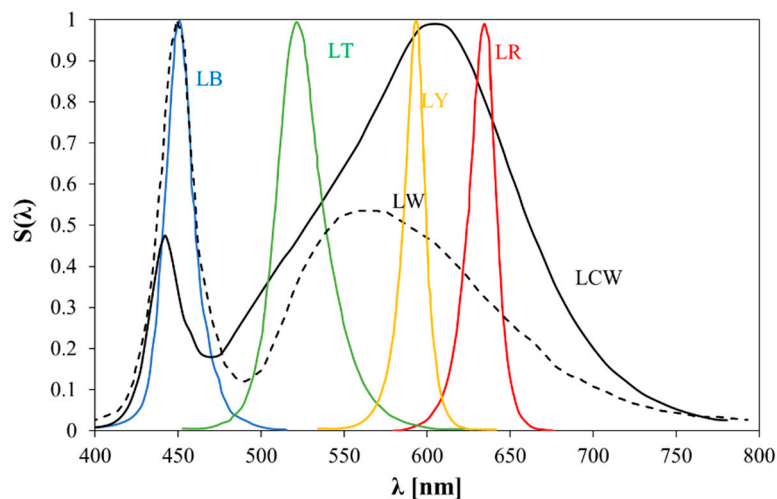


Figure 2. Relative emission spectra of the considered power LEDs.

It is visible that the presented relative emission spectra for the red and yellow diodes are very narrow, and their FWHM (Full Width at Half Maximum) is from 15 to 20 nm. The other diodes have wider spectra. For blue and green diodes the FWHM is from 30 to 40 nm. Of course, the widest spectra were measured for the LEDs emitting white light. For these diodes, two maxima are observed in the range of blue light and yellow-green light.

All the tested diodes use the same lens. Therefore, they have the same emission characteristics shown in Figure 3. These characteristics can be approximated with the square function. As can be observed, the maximum emission angle α_{max} is equal to 85° .

The investigated power LEDs are assembled in identical cases and soldered in the same process to the same PCB of the dimensions 100×100 mm with the basis FR-4 which is glass-reinforced epoxy laminate material. It is a composite material composed of woven fiberglass cloth with an epoxy resin binder that is flame resistant. This PCB is 1.5 mm thick and contains an internal copper layer. This layer is used as the electrical connection between the anodes of all the LEDs. The tested diodes are situated

in two rows lying at a distance of 18 mm from each other. In each row, the distance between the diodes is equal to 30 mm.

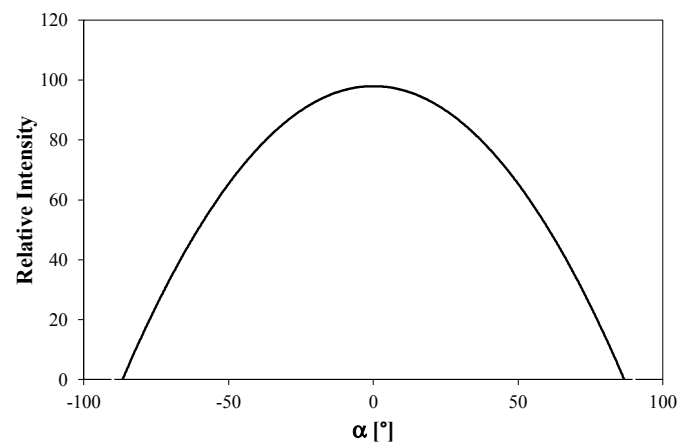


Figure 3. The catalog emission characteristic of the considered power LEDs.

3. Measurements Set-Ups and Methods

Selected characteristics of the considered devices were measured with the use of two measurement set-ups. The first is dedicated to measuring the properties of the diodes operating separately. The diagram of this set-up is shown in Figure 4. The other set-up, shown in Figure 5, makes it possible to measure the characteristics of the tested devices with mutual thermal couplings taken into account. Figure 6 contains a photo of the measurement set-up of the diagram shown in Figure 5.

With the use of the set-up shown in Figure 4, dc current-voltage characteristics of the tested diodes can be measured at a thermally steady state and such parameters of these diodes as transient thermal impedance, illuminance and the surface power density of the emitted light. In order to eliminate the influence of other lighting sources on the results of measurements, the tested diodes are situated in a light-tight chamber of the dimensions, $400 \times 250 \times 220$ mm. In turn, a precision luxmeter and a radiometer are used to measure illuminance and the surface power density of the emitted light, respectively. These measurements can be realized at the steady state and at the transient state. Probes of the radiometer and the luxmeter are situated in the axis of the tested diodes. Therefore, measurements with the use of the mentioned instruments cannot be performed at the same time. A radiometer of the type HD2302 by DeltaOhm [43] and the precision luxmeter L-100 by Sonopan [44] were used. According to the user manual of the radiometer [43], this radiometer can measure radiation of a spectral range from 400 to 1050 nm with calibration uncertainty smaller than 5%. In turn, the used precision luxmeter L-100 was calibrated by the manufacturer and its accuracy is characterized by class A by CIE.

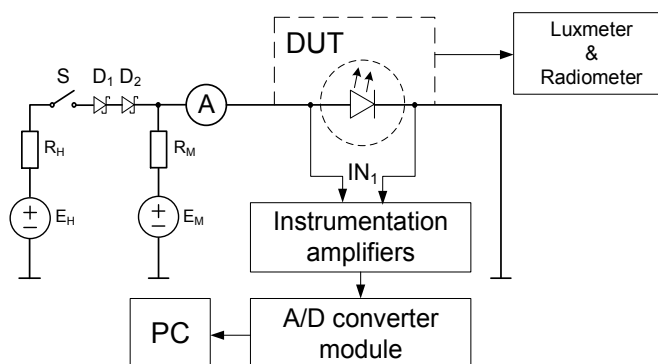


Figure 4. Diagram of the measuring set-up dedicated to a single diode.

The considered set-up makes it possible to measure real transient thermal impedance as defined in the paper [45]. In the definition of this parameter, it is taken into account that only a part of dissipated power (heating power) causes self-heating phenomena and the other part of this power (optical power) is converted into light.

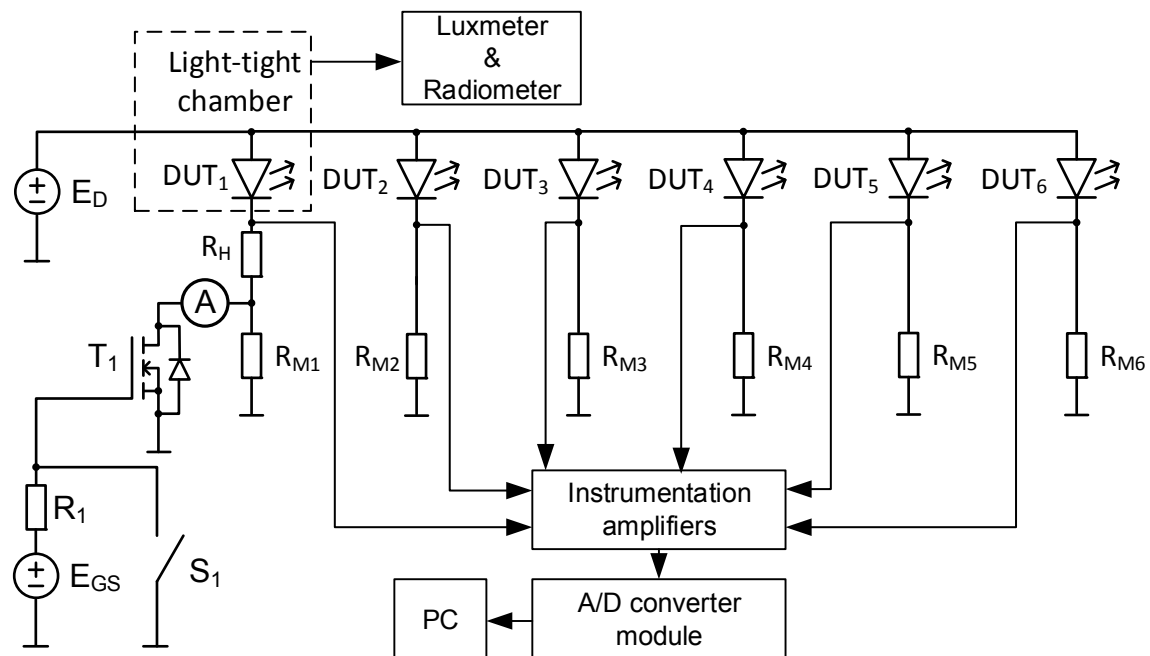


Figure 5. Diagram of the measurement set-up dedicated to thermally coupled diodes.



Figure 6. The view of the measurement set-up of the diagram in Figure 5.

The indirect electrical method is used to measure transient thermal impedance. One can find a detailed description of this method in the paper [27].

This method uses forward voltage V_F of the diode biased with a current of a small value I_M as a thermo-sensitive parameter. The value of such a parameter nearly linearly depends on the device internal temperature [46–48]. Measurements of the device internal temperature are realized in three steps. At first, the thermometric characteristic $V_F(T)$ is measured at the fixed value of the diode forward current I_M . In this step of measurements, switch S is opened and the diode is situated in a thermal chamber the temperature of which can be regulated. In the second step of measurements, switch S is closed and the internal temperature of the diode increases as a result of self-heating phenomena connected with current I_H flowing through the diode. At the thermally steady state, the diode current I_H is measured using the ammeter, forward voltage V_H is measured with the A/D converter module, illuminance with the luxmeter and the surface power density of the emitted light with the radiometer. Waveforms of the diode forward voltage are recorded using instrumentation amplifiers, the A/D converter module and a PC, whereas the heating current is measured using the ammeter. In the third step, immediately after switching off switch S , current I_M flows through the diode and the diode forward voltage V_C is measured. Using the measured waveform of forward voltage $V_C(t)$ and the thermometric characteristic $V_F(T)$, the value of the waveform of internal temperature $T_j(t)$ is determined. Finally, transient thermal impedance is determined with the use of the following formula:

$$Z_{th}(t) = \frac{T_j(t) - T_a}{V_H \cdot I_H - P_{opt}} \quad (1)$$

The value of optical power P_{opt} is determined with the use of the method described in [38,41]. In this method, in order to measure the value of optical power P_{opt} of the investigated power LEDs at the steady state one should [38,41]:

1. measure the surface optical power density E_e using the radiometer situated at a distance r from the surface of the LED at the end of the second step of the measurements,
2. calculate the average value of the relative surface optical power density $\overline{a_{opt}}$ using the catalog emission characteristics (dependence of relative intensity on the angle of observation α),
3. calculate optical power P_{opt} using the following formula [49]:

$$P_{opt} = E_e \cdot 2\pi \cdot r^2 \cdot (1 - \cos \alpha_{max}) \cdot \overline{a_{opt}} \quad (2)$$

In the paper [50], it was shown that the results of measurements obtained with the use of the described measurement set-up are practically the same as the results obtained with the use of a standard T3Ster instrument [51].

In turn, in order to measure mutual transient thermal impedances of the considered diodes, the set-up shown in Figure 5 was used.

In the set-up shown in Figure 5, only one diode (DUT_1) plays the role of a heater, whereas the other diodes are temperature sensors. In this set-up, E_D is the power supply voltage of the output voltage equal to 14.5 V. Devices denoted as DUT_1 – DUT_6 are the tested power LEDs. Resistors R_H and R_{M1} – R_{M6} are used to regulate the heating current I_H and to measure the current I_M of each diode. Voltage source E_{GS} is used to drive the gate of power MOSFET T_1 . Resistor R_1 limits the value of the gate current while switching transistor T_1 . Switch S_1 is open while heating diode DUT_1 and closed while cooling it.

Measurements of mutual transient thermal impedance are realized in the three steps described above, but in the third step of measurement, values of the forward voltage of all the diodes are registered. The mutual transient thermal impedance between diode DUT_1 and one of the other diodes DUT_i is determined with the use of the Formula (1), in which instead of $T_j(t)$ temperature, the junction temperature of the diode DUT_i must be used, whereas V_H and I_H correspond to the forward voltage of diode DUT_1 at a forward current of the diode I_H . P_{opt} is the optical power of the light emitted by

diode DUT₁. In order to measure all mutual transient thermal impedances, six measurement cycles should be performed. In each cycle, any diode of the other diodes is used as a heater DUT₁.

4. Measurements Results

The measurements of thermal and optical parameters of power LEDs described in Section 2 were performed with the use of the measuring set-ups described in Section 3. Some results of the performed measurements are presented in Figures 7–17.

Figure 7 illustrates the measured dependences of the forward voltage of the selected tested diodes on the temperature at a low value of forward current $I_F = 10$ mA. During the measurements, the considered power LEDs were situated in the thermal chamber, which stabilized the value of temperature with the error not higher than ± 2 K.

It is visible that the considered dependences $V_F(T)$ are practically linear. The slope of the measured characteristics falls in a range from -2.652 mV/K for the LB diode to -1.373 mV/K for the LW diode. The measured values of forward voltage were highest for the LB diode and lowest for the LY diode. Differences in values of forward voltage are observed due to differences in the band-gap of materials used to construct the dies of the tested power LEDs. Using the obtained results of measurements and the formula proposed in the paper [18], values of the band-gap of the tested diodes were calculated. These values for the tested diodes fall in a range from 2.04 to 3.37 eV. Such values correspond to the semiconductor materials typically used to construct power LEDs.

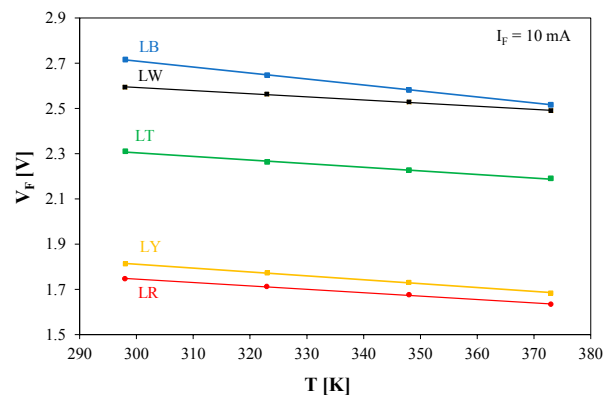


Figure 7. Calibration curves of selected power LEDs.

Figure 8 illustrates the measured waveforms of transient thermal impedance $Z_{th}(t)$ of the tested power LEDs obtained at forward current $I_F = 1$ A (Figure 8a) and the dependence of thermal resistance on the central wavelength λ of the spectrum of the emitted radiation (Figure 8b).

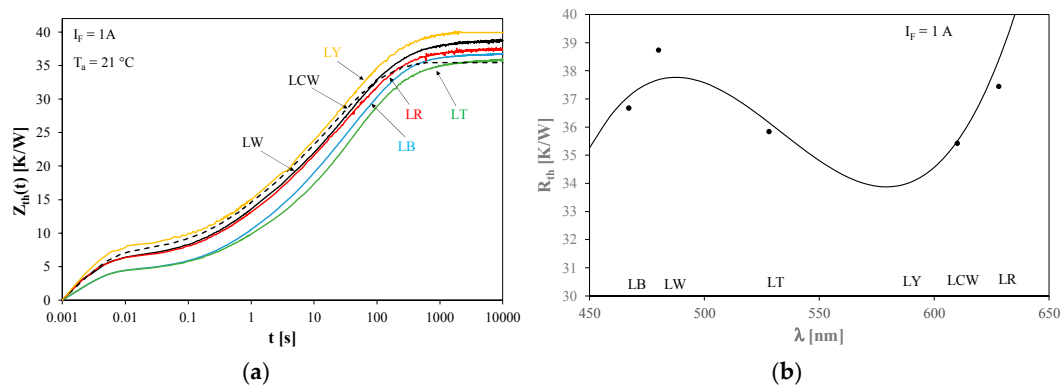


Figure 8. Measured waveforms of $Z_{th}(t)$ of the tested LEDs (a) and the dependence of thermal resistance on the central wavelength λ of the spectrum of the emitted radiation (b).

As visible in Figure 8a, the thermally steady state for all the diodes is observed for the time $t \approx 2000$ s. At the steady state, visible differences between values of transient thermal impedance (equal to thermal resistance R_{th}) for the tested power LEDs are observed. Values of thermal time constants describing each of the measured waveforms of $Z_{th}(t)$ were estimated using the method described in the paper [25]. For each of the considered devices, seven thermal time constants of values from 2.3 ms to 1800 s were obtained. These thermal time constants characterize particular components of the heat flow path of these power LEDs—from the semiconductor die to the PCB.

In turn, Figure 8b shows that thermal resistance visibly depends on the color of the emitted light. The highest value of thermal resistance, equal to about 39.9 K/W, is observed for the LY diode, whereas the lowest value of R_{th} is obtained for the LT and LCW diodes. Differences between values of R_{th} for the mentioned diodes even reach 15%. These differences result from differences in thermal power dissipated in the considered diodes and the influence of the device internal temperature on their thermal resistance described, for example, in [52]. The results of the measurements (points) can be correctly approximated (line) with the use of a polynomial of the third degree.

Additionally, we performed measurements of waveforms of transient thermal impedance and values of thermal resistance of all the tested power LEDs operating at different values of forward current. For example, Figure 9 shows the measured dependences of thermal resistance R_{th} of these LEDs on forward current I_F .

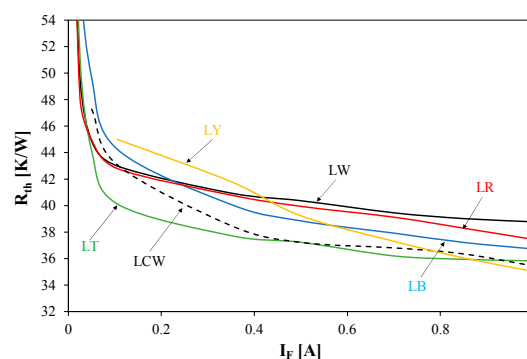


Figure 9. Measured dependences of thermal resistance of the tested diodes on forward current.

For all the tested diodes, the dependence $R_{th}(I_F)$ is a decreasing function. The slope of this dependence decreases with an increase in the current I_F . This slope is different for each of the diodes. For example, for the LT diode in the range of changes in the value of current I_F between 0.1 A and 1 A, the value of R_{th} decreases even by 10%. According to the considerations presented in the paper [53], values of R_{th} obtained at low values of current I_F could be characterized by a big measurement error.

Figure 10 illustrates the dependences of the temperature of the soldering points of the tested LEDs on their forward current. The temperature of the soldering point T_S and ambient temperature T_a were measured with the use of thermocouples.

As can be observed, for each diode dependence $T_S(I_F)$ is an increasing function. Differences between the results obtained for different diodes increase with an increase of forward current and they are equal to even 15 °C. They result from differences: in the diode forward voltage and in the efficiency of conversion of electrical energy into light of the tested diodes.

Figure 11 shows the measured dependences of the surface power density E_e of the emitted light on forward current. The measurements were performed at the thermally steady state with the use of the radiometer. The probe of the radiometer was situated in the axis of the tested diode in the distance $r = 17$ cm.

As visible, the considered dependence is an increasing function in a wide range of forward current. Only for the LR and LY diodes the maximum at forward current equal to $I_F = 0.8$ A was observed. Values of the surface power density E_e measured for the same value of current I_F differ from one another by even 10 times. The highest value of E_e was obtained for the LB diode. In turn, the lowest

value of this parameter was measured for the LY diode. The presented results of the measurements show that a high value of the emitted optical power can be more easily obtained for blue light than for other colors of the emitted light. It is also worth noticing that for diodes emitting neutral white light values of E_e are even twice as high as for such devices emitting warm white light. The observed differences in E_e for the considered power LEDs are a result of the dependence of internal quantum efficiency on the wavelength of the emitted light [3].

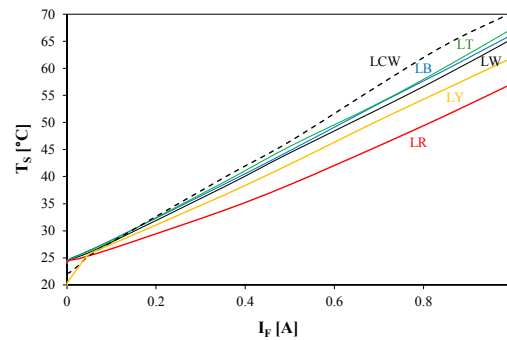


Figure 10. Measured dependences of the temperature of the soldering point T_s of the tested power LEDs on forward current.

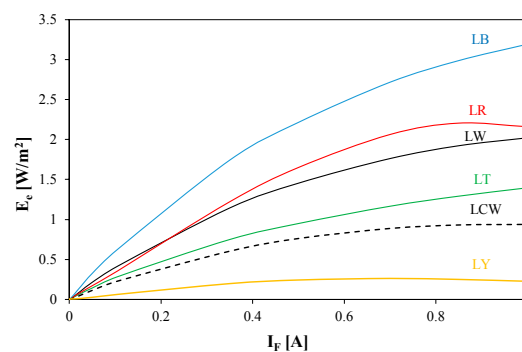


Figure 11. Measured dependences of the surface power density on forward current.

Figure 12 illustrates the dependences of the surface power density of the surface illuminated by the considered diodes on the central wavelength λ of the spectrum of the emitted radiation. The measurements were performed at selected values of forward current. In this figure, blue points denote the results obtained at current $I_F = 25$ mA, red points at $I_F = 0.35$ A and black points at $I_F = 1$ A.

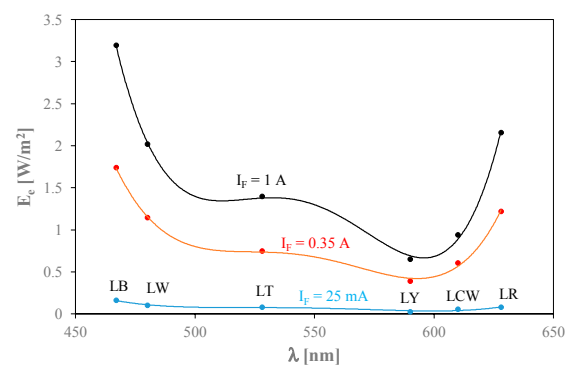


Figure 12. Measured and calculated dependences of the surface power density on the surface illuminated by the tested LEDs on the central wavelength λ of the spectrum of the emitted radiation for selected values of forward current of these diodes.

As visible, values of parameter E_e measured at the same value of current I_F for the considered diodes visibly differ from one another. These differences can even be triple. The highest values of parameter E_e are obtained for the LB diode, whereas the lowest for the LY diode. For each of the tested diodes, an increase in the value of forward current causes an increase in the value of E_e . When this current increases 40 times the surface power density increases only 16 times. The presented results show that it is easier to obtain a high value of the surface power density of the emitted light in the range of blue light than in the range of green, red, white or yellow light.

On the basis of the obtained results of measurements, the analytical dependence $E_e(\lambda)$ in the form of a polynomial of fourth degree was proposed. The coefficients existing in this formula depend on the value of the forward current. Dependences calculated with the use of the elaborated formula are marked in Figure 12 with lines. As visible, very good agreement between the results of measurements and calculations was obtained.

Figure 13 shows the dependences of the optical efficiency η_{opt} of the tested power LEDs on their forward current. Optical efficiency is defined as the quotient of the optical power of the emitted light and electrical power consumed by the considered diode. A high value of watt-hour efficiency of the conversion of electrical energy into light η_{opt} is very important for designers and users of the considered semiconductor devices.

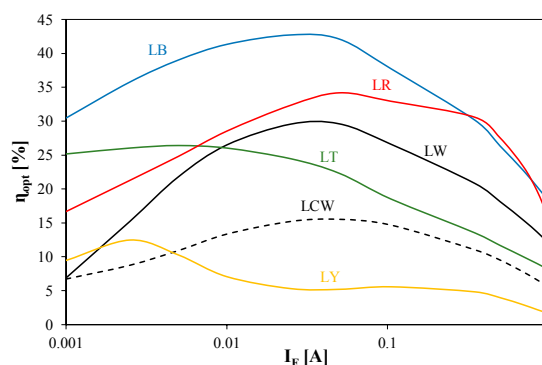


Figure 13. Measured dependences of optical efficiency of the tested power LEDs on forward current.

It is easy to observe that the considered dependences possess the maximum value at forward current $I_F \approx 25$ mA. The highest value of parameter η_{opt} can be observed for the LB diode. This value even reaches 43%. In contrast, the maximum value of optical efficiency obtained for the LY diode is equal to only 13%. In the range of high values of forward current, exceeding 200 mA, the highest value of optical efficiency is observed for the LR diode. It can be noticed that an increase in the value of forward current in the range from 25 mA to 1 A causes even a double decrease in the value of optical efficiency. This relation shows that in order to obtain a high value of optical efficiency the tested power LEDs should operate at values of forward current much lower than their maximum allowable value declared by the producer.

Figure 14 shows waveforms of illuminance E_V measured on the surface illuminated by the considered LEDs excited with a step of forward current of the value equal to 1 A. The measurements were performed with the use of a probe of the luxmeter situated in the axis of the tested diodes and at a distance between them equal to 17 cm.

As can be observed, the obtained waveforms $E_V(t)$ are decreasing functions of time. This is a result of self-heating phenomena occurring in these power LEDs. Values of illuminance at the steady state are highest for the LT diode and lowest for the LY diode. The obtained values of this parameter at the steady state differ from one another for the tested diodes even five times. The observed differences are a result of the quantum efficiency of the tested devices and the spectrum characteristic of the sensitivity of the human eye. This sensitivity has the highest values for green light. Due to the various spectra of the emitted light produced by each diode and the spectra of the sensitivity of the human eye,

relations between values of illuminance of the considered diodes are different than relations of the surface power density characterizing the light emitted by the same diodes.

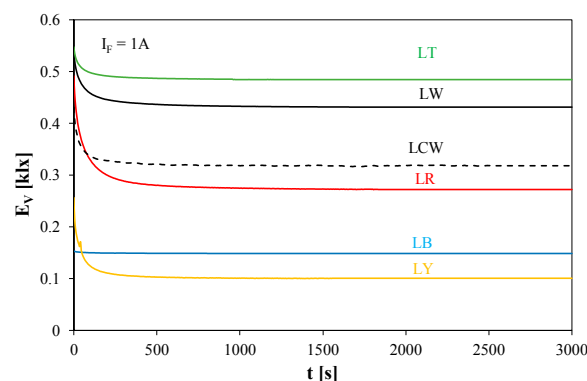


Figure 14. Waveforms of illuminance measured when exciting the tested diodes by a step of current.

Measurements, the results of which are shown in Figures 7–14, were performed while feeding one tested diode only. Other diodes were not fed. In contrast, Figures 15–17 illustrate the influence of mutual thermal couplings on the thermal and optical properties of the tested diodes.

Figure 15 illustrates waveforms of self and transfer transient thermal impedances of the tested power LEDs measured using the set-up shown in Figure 5. Measurements were performed while heating the LT diode (Figure 15a) and the LY diode (Figure 15b). The LT diode was situated in the middle of the PCB including all the diodes, whereas the LY diode was close to the border of this PCB.

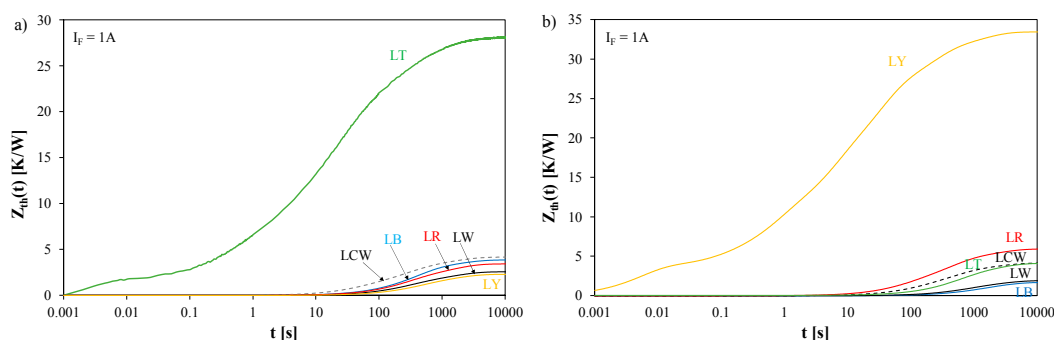


Figure 15. Measured waveforms of self and transfer transient thermal impedances of the tested diodes obtained while heating the LT diode (a) or LY diode (b).

As visible, self-transient thermal impedances of the tested diodes differ by even 10% from one another. A higher value of this parameter is observed for the LY diode situated near the border of the PCB. It is worth noticing that transfer transient thermal impedances are much lower (even 15 times) than self-transient thermal impedances. The waveforms of mutual transient thermal impedances depend on the distance between the thermally coupled diodes. An increase in the distance between such diodes causes a decrease in the value of mutual thermal resistance and an increase in time indispensable to obtain the thermally steady state. For the diodes situated at the same distance from the heating diode, nearly the same waveforms of transfer thermal impedance were obtained.

Figure 16 illustrates waveforms of internal temperatures of all the diodes while cooling after obtaining the thermally steady state at a simultaneous power supply. The value of current I_F for each diode is equal to 750 mA.

The measured values of temperature T_j for the tested diodes differ visibly from one another. The observed differences exceed even 30 °C. This means that visible non-uniformities in temperature distribution on the PCB are observed and the use of only one value of temperature characterizing

the whole PCB of the tested devices could result in high values of errors in the estimation of such temperature. It is also worth noticing that at forward current much lower than allowable, the value of junction temperature of selected diodes could be higher than their maximum allowable value due to self-heating and mutual thermal couplings between the devices operating on the common PCB.

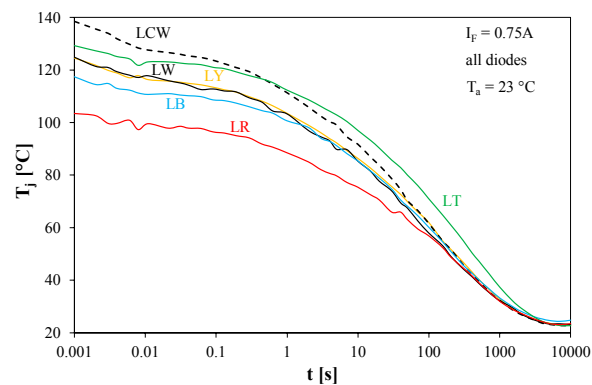


Figure 16. Measured waveforms of internal temperature of all the tested power LEDs while cooling after power supplying all the diodes.

In order to illustrate the influence of mutual thermal couplings on thermal and optical properties of the tested power LEDs, values of junction temperature T_j of these diodes and the surface power density E_e are measured in two cases. In the first case (denoted with red color), current $I_F = 750$ mA flows through one tested diode only. In the other case (denoted with green color), this current flows simultaneously through all the diodes. The results obtained at the steady state are shown in Figure 17. During the measurements of E_e , the probe of the radiometer was situated in the distance $r = 3.5$ cm from the tested diode.

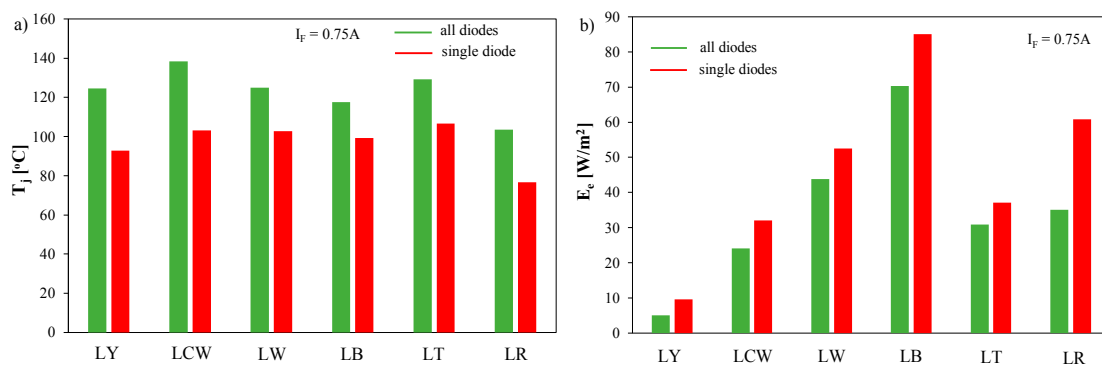


Figure 17. Measured values of junction temperature (a) and the surface power density of the emitted light (b) for power LEDs operating alone and simultaneously with all other diodes.

In Figure 17a, it is easy to observe that the power supply of the other diodes causes an additional increase in junction temperature. This increase is lowest for the LB diode (equal to 20 °C) and highest for the LCW diode (equal to 40 °C). As a result of an increase in junction temperature, a decrease in E_e is observed in Figure 17b. The biggest decrease occurs for the LR diode. It is equal to even 40%. The measurement results presented above prove that mutual thermal couplings between power LEDs situated on the common PCB could visibly and unfavorably influence values of the device junction temperature and parameters characterizing the emitted light.

5. Conclusions

This paper presents measurement results illustrating the influence of the spectra of the emitted light on selected optical and thermal parameters of power LEDs operating on the common PCB. All the tested devices are assembled in the same type of cases and soldered in the same process. The measurements were performed for diodes emitting monochromatic light (blue, red, green or yellow) or white light characterized by different values of CCT. The dies used to construct the tested devices were made of different semiconductor materials.

In contrast to the results presented by the producer, in our investigations, the thermal phenomena occurring in the tested devices were taken into account. There are self-heating and mutual thermal couplings between each pair of diodes operating on the common PCB. As a result of thermal phenomena, the measured values of optical parameters visibly differ from values given by the producer in the catalog data and the junction temperature of each diode can be much higher than the ambient temperature.

The results of the performed measurements prove that the spectra of the emitted light strongly influence such optical parameters of power LEDs as optical efficiency, illuminance and the surface power density on the surface illuminated by the tested diodes. The results of measurements of the mentioned parameters obtained for power LEDs emitting light of different spectra differ from one another by even 10 times. Radiometric parameters have the highest values for the diode emitting blue light, whereas photometric parameters are highest for the diode emitting green light. This is a result of both the physical properties of the used semiconductor dies and the spectra characteristic of the sensitivity of the human eye. Dependences of the mentioned optical parameters and thermal resistance on the central wavelength λ of the spectrum of the emitted radiation can be effectively described with the use of polynomial functions.

Analyzing the measured dependences of selected optical parameters on forward current, one can easily notice that the most favorable is the operation of the tested devices at forward current of a value much lower than the maximum allowable value given by the producer. A decrease in the value of optical efficiency at an increase in the forward current can reach even 50%.

The spectra of the emitted light visibly influence the value of thermal resistance of the tested devices. This parameter can have values which differ even by about 10% between the tested diodes. These differences could be a result of the different places of mounting for these devices on the PCB and the distance between the tested power LED and the border of the PCB. It is also worth noticing that for the considered diodes operating alone at the same value of forward current, big differences in the junction temperature of the tested devices were obtained. These differences can even exceed 30 °C. Therefore, during the formulation of a thermal model of solid state lighting sources, the junction temperature of each diode should be calculated separately.

The applied method of mounting the tested diodes limits the maximum value of the junction temperature of the tested devices to about 110 °C. It was also noticed that the differences between this temperature and the temperature of the soldering point can be higher than even 40 °C. Therefore, in order to obtain a long lifetime for the tested devices, efficient heat removal from the soldering point is needed.

In turn, the measurements performed for all the tested diodes operating together illustrate that mutual thermal couplings between power LEDs situated on the common PCB can visibly change the value of junction temperature of the tested diodes. In the case when all the diodes operate together, this temperature can be higher even by 40 °C than in the case when the diode operates alone with the same value of forward current. This increase in junction temperature T_j also causes a visible decrease in the surface power density E_e . Changes in values of T_j and E_e strongly depend on the color of the emitted light. They are lowest for the diode emitting blue light and highest for the diodes emitting yellow or red light. The changes in the values of E_e caused by mutual thermal couplings can exceed even 50%. Therefore, while modeling properties of solid state lighting sources, mutual thermal couplings between power LEDs situated on the common PCB should be taken into account.

The results of investigations presented in this paper are obtained for one family of power LEDs only, but the obtained relations between electrical, optical and thermal parameters of these devices have a universal character. The influence of self-heating and mutual thermal couplings on optical and thermal parameters of power LEDs is characterized by decreasing functions of thermal power and the distance between the thermally coupled devices. Additionally, the spectra of the emitted light influence self and transfer thermal resistances of the tested power LEDs.

The obtained results of investigations could be usable for designers of solid-state lighting sources, including power LEDs, emitting light of different colors. They can be also used as teachings to illustrate the influence of the spectra of the emitted light and thermal phenomena on the properties of selected lighting sources. In the near future, we will propose a computer model of power LEDs that will take into account the properties of the devices presented in this paper.

Author Contributions: Conceptualization (K.G. and P.P.); methodology (K.G. and P.P.); investigation (P.P.); writing—original draft preparation (K.G.); writing—review and editing (K.G. and P.P.); visualization (K.G. and P.P.); supervision (K.G.). All authors have read and agreed to the published version of the manuscript.

Funding: This research was funded by the program of the Ministry of Science and Higher Education called “Regionalna Inicjatywa Doskonałości” in the years 2019–2022, project number 006/RID/2018/19, sum of financing 11 870 000 PLN.

Conflicts of Interest: The authors declare no conflict of interest.

References

1. Weir, B. Driving the 21st Century’s Lights. *IEEE Spectr.* **2012**, *49*, 42–47. [\[CrossRef\]](#)
2. Huang, J.; Kuo, H.C.; Shen, S.C. *Nitride Semiconductor Light-Emitting Diodes (LEDs)*, 2nd ed.; Elsevier: Cambridge, UK, 2018.
3. Schubert, E.F. *Light Emitting Diodes*, 2nd ed.; Cambridge University Press: New York, NY, USA, 2008.
4. Górecki, K.; Ptak, P. Modelling LED lamps in SPICE with thermal phenomena taken into account. *Microelectron. Reliab.* **2017**, *79*, 440–447. [\[CrossRef\]](#)
5. Narendran, N.; Gu, Y. Life of LED-based white light sources. *J. Disp. Technol.* **2005**, *1*, 167–171. [\[CrossRef\]](#)
6. Lasance, C.J.M.; Poppe, A. *Thermal Management for LED Applications*; Springer Science + Business Media: New York, NY, USA, 2014.
7. Janicki, M.; Starzak, Ł.; Torzewicz, T.; Ptak, P.; Górecki, K. Thermal characterisation of colour power LEDs. In Proceedings of the 26th International Conference Mixed Design of Integrated Circuits and Systems MIXDES, Rzeszów, Poland, 27–29 June 2019; pp. 283–286.
8. Liu, S.M.; Chou, Y.C. Color Calibration for a Surrounding True-Color LED Display System by PWM Controls. *IEEE Trans. Ind. Electron.* **2014**, *61*, 6244–6252. [\[CrossRef\]](#)
9. Poppe, A.; Farkas, G.; Szekely, V.; Horvath, G.; Rencz, M. Multi-domain simulation and measurement of power LEDs and power LED assemblies. In Proceedings of the 22nd Annual IEEE Semiconductor Thermal Measurement and Management Symposium, Dallas, TX, USA, 14–16 March 2006; pp. 191–198.
10. Li, K.H.; Cheung, Y.F.; Jin, W.; Fu, W.Y.; Lee, A.T.L.; Tan SCh Hui, S.Y.; Choi, H.W. InGaN RGB Light-Emitting Diodes with Monolithically Integrated Photodetectors for Stabilizing Color Chromaticity. *IEEE Trans. Ind. Electron.* **2020**, *67*, 5154–5160. [\[CrossRef\]](#)
11. Lee, A.T.L.; Chen, H.; Tan, S.; Hui, S.Y. Precise Dimming and Color Control of LED Systems Based on Color Mixing. *IEEE Trans. Power Electron.* **2016**, *31*, 65–80. [\[CrossRef\]](#)
12. Chen, H.; Tan, S.; Hui, S.Y. Nonlinear dimming and correlated color temperature control of bicolor white LED systems. *IEEE Trans. Power Electron.* **2015**, *30*, 6934–6947. [\[CrossRef\]](#)
13. Hui, S.Y.; Qin, Y.X. A General Photo-Electro-Thermal Theory for Light Emitting Diode (LED) Systems. *IEEE Trans. Power Electron.* **2009**, *24*, 1967–1976. [\[CrossRef\]](#)
14. Tao, X.; Hui, S.Y.R. Dynamic Photoelectrothermal Theory for Light-Emitting Diode Systems. *IEEE Trans. Ind. Electron.* **2012**, *59*, 1751–1759. [\[CrossRef\]](#)
15. Tao, X.; Chen, H.; Li, S.N.; Hui, S.Y.R. A New Noncontact Method for the Prediction of Both Internal Thermal Resistance and Junction Temperature of White Light-Emitting Diodes. *IEEE Trans. Power Electron.* **2012**, *27*, 2184–2192. [\[CrossRef\]](#)

16. Hui, S.Y.; Lee, A.T.L.; Tan, S. New Dynamic Photo-Electro-Thermal Modeling of Light-Emitting Diodes with Phosphor Coating as Light Converter Part I: Theory, Analysis, and Modeling. *IEEE J. Emerg. Sel. Top. Power Electron.* **2020**, *8*, 771–779. [\[CrossRef\]](#)
17. Lee, A.T.L.; Chen, H.; Tan, S.; Hui, S.Y. New Dynamic Photo-Electro-Thermal Modeling of Light-Emitting Diodes With Phosphor Coating as Light Converter—Part II: Model Parameter Determination and Practical Verification. *IEEE J. Emerg. Sel. Top. Power Electron.* **2020**, *8*, 780–793. [\[CrossRef\]](#)
18. Chen, H.; Lee, A.T.L.; Tan, S.; Hui, S.Y. Dynamic Optical Power Measurements and Modeling of Light-Emitting Diodes Based on a Photodetector System and Photo-Electro-Thermal Theory. *IEEE Trans. Power Electron.* **2019**, *34*, 10058–10068. [\[CrossRef\]](#)
19. Górecki, K. Modelling mutual thermal interactions between power LEDs in SPICE. *Microelectron. Reliab.* **2015**, *55*, 389–395. [\[CrossRef\]](#)
20. Mawby, P.A.; Iqic, P.M.; Towers, M.S. Physically based compact device models for circuit modelling applications. *Microelectron. J.* **2001**, *32*, 433–447. [\[CrossRef\]](#)
21. Biber, C. LED light emission as a function of thermal conditions. In Proceedings of the 24th IEEE Semiconductor Thermal Measurement and Management Symposium SEMI-THERM, San Jose, CA, USA, 16–20 March 2008; pp. 180–184.
22. Górecki, P.; Górecki, K. Modelling dc characteristics of the IGBT module with thermal phenomena taken into account. In Proceedings of the 13th IEEE International Conference on Compatibility, Power Electronics and Power Engineering IEEE CPE POWERENG 2019, Sonderborg, Denmark, 23–25 April 2019.
23. Poppe, A. Simulation of LED based luminaries using their multi-domain compact models and CTMs of their thermal environment. *Microelectron. Reliab.* **2017**, *72*, 65–74. [\[CrossRef\]](#)
24. Farkas, G.; Bein, M.C.; Gaal, L. Multi domain modelling of power LEDs based on measured isothermal and transient I-V-L characteristics. In Proceedings of the 22nd International Workshop on Thermal Investigations of ICs and Systems Thermisic, Budapest, Hungary, 21–23 September 2016; pp. 181–186.
25. Górecki, K.; Zarebski, J.; Górecki, P.; Ptak, P. Compact thermal models of semiconductor devices—A review. *Int. J. Electron. Telecommun.* **2019**, *65*, 151–158.
26. Górecki, K.; Detka, K. Application of average electrothermal models in the SPICE-aided analysis of boost converters. *IEEE Trans. Ind. Electron.* **2019**, *66*, 2746–2755. [\[CrossRef\]](#)
27. Górecki, K.; Ptak, P. New method of measurements transient thermal impedance and radial power of power LEDs. *IEEE Trans. Instrum. Meas.* **2020**, *69*, 212–220. [\[CrossRef\]](#)
28. Górecki, K.; Ptak, P. The influence of the mounting manner of the power LEDs on its thermal and optical parameters. In Proceedings of the 21st International Conference Mixed Design of Integrated Circuits and Systems MIXDES, Lublin, Poland, 19–21 June 2014; pp. 303–308.
29. Janicki, M.; Torzewicz, T.; Samson, A.; Raszowski, T.; Napieralski, A. Experimental identification of LED compact thermal model element values. *Microelectron. Reliab.* **2018**, *86*, 20–26. [\[CrossRef\]](#)
30. Barnea, S.N.; Sciuto, G.L.; Hai, N.; Shikler, R.; Capazzi, G.; Woźniak, M.; Połap, D.L. Photo-electro characterization and modeling of organic light-emitting diodes by using a radial basis neural network. In *International Conference on Artificial Intelligence and Soft Computing*; Springer: Berlin, Germany, 2017; pp. 378–389.
31. Zhao, M.; Zhong, S.; Fu, X.; Tang, B.; Pecht, M. Deep residual shrinkage networks for fault diagnosis. *IEEE Trans. Ind. Inform.* **2020**, *16*, 4681–4690. [\[CrossRef\]](#)
32. Driel, W.D.; Fan, X.J. *Solid State Lighting Reliability, Components to Systems*; Springer Science + Business Media: New York, NY, USA, 2013.
33. Chang, M.H.; Das, D.; Varde, P.V.; Pecht, M. Light emitting diodes reliability review. *Microelectron. Reliab.* **2012**, *52*, 762–782. [\[CrossRef\]](#)
34. Schweitzer, D.; Ender, F.; Hantos, G.; Szabo, P.G. Thermal transient characterization of semiconductor devices with multiple heat-sources—Fundamentals for a new thermal standard. *Microelectron. J.* **2015**, *46*, 174–182. [\[CrossRef\]](#)
35. Górecki, K.; Górecki, P.; Zarebski, J. Measurements of parameters of the thermal model of the IGBT module. *IEEE Trans. Instrum. Meas.* **2019**, *68*, 4864–4875. [\[CrossRef\]](#)
36. Ptak, P.; Górecki, K.; Dziurdzia, B. Modelling thermal properties of large LED module. *Mater. Sci. Pol.* **2019**, *37*, 628–638. [\[CrossRef\]](#)

37. Ozluk, B.; Muslu, A.M.; Arik, M. A Comparative Study for the Junction Temperature of Green Light Emitting Diodes LEDs. *IEEE Trans. Compon. Packag. Manuf. Technol.* **2019**, *9*, 2024–2035. [CrossRef]
38. Górecki, K.; Ptak, P. New dynamic electro-thermo-optical model of power LEDs. *Microelectron. Reliab.* **2018**, *91*, 1–7. [CrossRef]
39. Górecki, K.; Ptak, P. Influence of the wavelength of emitted radiation on thermal and radiometry parameters of selected power LEDs. In Proceedings of the 25 International Workshop on thermal Investigations of ICs and Systems Thermic 2019, Lecco, Italy, 25–27 September 2019.
40. W5SM LED type Golden DRAGON OSRAM Opto Semiconductors. Available online: www.osram-os.com (accessed on 20 March 2020).
41. Górecki, K.; Ptak, P.; Janicki, M.; Torzewicz, T. Influence of cooling conditions of power LEDs on their electrical, thermal and optical parameters. In Proceedings of the 25th International Conference Mixed Design of Integrated Circuits and Systems MIXDES 2018, Gdynia, Poland, 21–23 June 2018; pp. 237–242.
42. Górecki, K.; Ptak, P. Influence of the area of a thermal pad on optical and thermal parameters of LED modules. *Circuit World* **2020**, *46*, 65–70. [CrossRef]
43. Datasheet DeltaOhm HD2302. Available online: <https://www.deltaohm.com/en/wp-content/uploads/document/DeltaOHM-2302.0-Portabe-Luxmeter-Datasheet-en.pdf> (accessed on 12 October 2020).
44. L-100 Precise Luxmeter Datasheet. Available online: <https://www.sonopan.com.pl/pl/produkty/swiatlo/luksomierz-precyzyjny-l-100/> (accessed on 22 June 2020).
45. JEDEC Standard JESD51-51. Implementation of Electrical Test Method for the Measurement of Light-Emitting Diodes. Available online: https://www.jedec.org/document_search?search_api_views_fulltext=StandardJESD51-51&order=title&sort=asc (accessed on 12 October 2020).
46. Blackburn, D.L. Temperature Measurements of Semiconductor Devices—A Review. In Proceedings of the 20th IEEE Semicon. Thermal Measurement and Management Symposium SEMI-THERM, San Jose, CA, USA, 11 March 2004; pp. 70–80.
47. JEDEC Standard JESD51-52. Guidelines for Combining CIE 127-2007 Total Flux Measurements with Thermal Measurements of LEDs with Exposed Cooling Surface. Available online: https://www.jedec.org/document_search?search_api_views_fulltext=Standard+JESD51-52 (accessed on 12 October 2020).
48. Avenas, Y.; Dupont, L.; Khatir, Z. Temperature measurement of power semiconductor devices by thermo-sensitive electrical parameters—A review. *IEEE Trans. Power Electron.* **2012**, *27*, 3081–3092. [CrossRef]
49. Dziurdzia, B.; Górecki, K.; Ptak, P. Influence of a soldering process on thermal parameters of large power LED modules. *IEEE Trans. Compon. Packag. Manuf. Technol.* **2019**, *9*, 2160–2167. [CrossRef]
50. Górecki, K.; Ptak, P.; Janicki, M. Comparison of set-ups dedicated to measure thermal parameters of power LEDs. In Proceedings of the 27th Internal Conference Mixed Design of Integrated Circuits and Systems Mixdes, Łódź, Poland, 25–27 June 2020; pp. 127–132.
51. Datasheet T3Ster Equipment. Available online: <https://corner-stone.com.tw/wp-content/uploads/2017/06/T3ster-technical-information.1.pdf> (accessed on 12 October 2020).
52. Górecki, K.; Górecki, P. Nonlinear compact thermal model of the IGBT dedicated to SPICE. *IEEE Trans. Power Electron.* **2020**, *35*, 13420–13428. [CrossRef]
53. Górecki, K.; Górecki, P. The analysis of accuracy of the selected methods of measuring thermal resistance of IGBTs. *Metrol. Meas. Syst.* **2015**, *22*, 455–464. [CrossRef]

